Analyst

Accepted Manuscript

This article can be cited before page numbers have been issued, to do this please use: R. Zhang, Y. Wang, X. Qu, S. Li, Y. Zhao, S. Liu, F. Zhang, J. Huang and J. Yu, *Analyst*, 2019, DOI: 10.1039/C9AN00857H.

View Article Online
DOI: 10.1039/C9AN00857H

A Label-free Electrochemical Platform for Antibiotics Detection Based on Cascade Enzymatic Amplification Coupled with Split G-quadruplex DNAzyme

Rufeng Zhang[a], Yu Wang[b], Xiaonan Qu[a], Shasha Li[b], Yihan Zhao[b], Fenfen Zhang[a], Su Liu[a], Jiadong Huang[b c] Jinghua Yu[c]*

a School of Water Conservancy and Environment, University of Jinan, Jinan 250022,P.R. China.

b College of Biological Sciences and Technology, University of Jinan, Jinan 250022, P.R. China.

c Key Laboratory of Chemical Sensing & Analysis in Universities of Shandong, College of Chemistry and Chemical Engineering, University of Jinan, Jinan 250022, P.R. China.

* Corresponding author. E-mail: stu_lius@ujn.edu.cn; Tel.: +86-531-89736122; Fax: +86-531-82769122.

View Article Online
DOI: 10.1039/C9AN00857H

Abstract

Herein, a split G-quadruplex DNAzyme as signal reporter has been integrated into electrochemical sensing for detecting antibiotic with specificity and sensitivity. To improve the signal-to-noise, the two G-rich oligonucleotide sequences (G1 and G2) are blocked into two different hairpin probes, respectively, preventing the two segments from assembling into the spilt G-quadruplex structure. Besides, we design a double-arch probe consisting of aptamer as the recognition element and two steps enzymatic signal amplification. Concretely, the first is the *Nt.BbvCI*-assisted nicking cyclic reaction activated by target-aptamer binding, and the second is an exonuclease III-aided cyclic amplification for generating abundant G1 and G2. The modified capture probe on the electrode is used to combine the G1 and G2 to form the spilt G-quadruplex/hemin when the K^+ and hemin are present. The complex plays a role of DNAzyme with superior horseradish peroxidase activity in catalyzing H_2O_2 decomposition. Under the optimal conditions, this biosensor shows excellent performance for kanamycin with detection limits of 83 fM ranging from 100 fM to 1 nM. Hence, the proposed strategy has the potential to develop an efficient and actual platform of small molecular analysis.

Keywords: spilt G-quadruplex DNAzyme; cascade signal amplification; electrochemical biosensor; antibiotic

View Article Online
DOI: 10.1039/C9AN00857H

Introduction

As is known to all, antibiotics, an effective drug resisted to pathogenic bacteria, have made outstanding contributions in the treatment of animal and human diseases[1-3]. However, excessive undegraded antibiotics are ingested to cause allergic reactions and induce the generation of antibiotic resistance gene, resulting in various types of side effects in humans and the appearance of super bacteria with tolerance to antibiotics[4-10]. Until now, many analytical ways for detecting antibiotics have been reported, such as high performance liquid chromatography (HPLC)[11], capillary electrophoresis (CE)[12], enzyme-linked immunosorbent assay (ELISA)[13], surface-enhanced Raman scattering (SERS)[14 15], surface plasmon resonance (SPR)[16], fluorescence resonance energy transfer (FRET)[17], etc. Regrettably, these conventional methods have suffered from such disadvantages as low selectivity, expensive instrumentation and complex operation procedures. Thereby, developing a rapid, reliable, and efficient detection method for antibiotics is urgent and significant. Alternatively, biosensor assay has been widely applied in detecting small molecule[18 19] as its merit of low cost, simplicity and high portability. Notably, there are two crucial constitutes for affecting the performance of the biosensor, namely recognition element and signal output reporter.

Aptamers, a kind of artificially synthesized oligonucleotides selected through systematic evolution of ligands by exponential enrichment (SELEX), can highly specific bind some small organic molecules and proteins[20-23]. Compared with antibodies, aptamers express obvious advantages containing predominant chemical stability, low fabrication cost and small size. Therefore, as recognition elements, aptamers have attracted more attention in electrochemical biosensing field for detecting various analytes, such as proteins[24], exosomal

View Article Online
DOI: 10.1039/C9AN00857H

microRNAs[25], heavy metal ions[26], with high sensitivity and selectivity. To achieve trace detection of the target, the signal amplification strategy is an essential part of fabricating the electrochemical biosensor, including enzyme-assisted recycling signal amplification, nanomaterial-mediated signal amplification and catalyzed hairpin assembly. Among these methods, the first strategy has obviously advantages contain multiple cycle steps and append additional reagent. As has been mentioned above, the enzyme-assisted amplification is an outstanding measure for improving sensitivity on account of its wonderful amplification efficiency and easy operation.

G-quadruplex, one of the typical DNA motifs which composed of a four-stranded structure with guanine (G)-rich DNA sequence, has widely served as an efficient signal transducing tool in biosensor strategies[27 28 29]. For instance, Guo's group employed the G-quadruplex/hemin as a signal reporter for *Pathogenic bacteria* detection[30]. Zhang et.al reported a photoelectrochemical strategy for disease marker detection based on RCA and Exo III amplification coupled with G-quadruplex/hemin.[31]. However, the developed G-quadruplex DNAzyme-based biosensors adopt independent anti-hemin aptamer as the catalytic tag, which maybe cause a low signal-to-noise (S/N). For surmounting this problem, the split G-quadruplex as a signal-transducing tool can replace the sole G-quadruplex. For example, Zhou and co-worker designed a label-free biosensor to detect T4 PNK activity by employing the split G-quadruplex[32]. Cui's work also used a spilt G-quadruplex DNAzyme as biocatalyst and developed a colorimetric method for analyzing antibiotic[33]. These mentioned spilt G-quadruplex DNAzyme strategies can effective avoid false positive signal and enhance the S/N, which is also associated with other analytical techniques such as electrochemical

View Article Online
DOI: 10.1039/C9AN00857H

biosensors.

Herein, we have reported a label-free electrochemical biosensor for ultrasensitive detection of antibiotics using enzyme-assisted cascade signal amplification coupled with split G-quadruplex DNAzyme strategy. As far as we know, this is the first time that split G-quadruplex DNAzyme has been applied in electrochemical field for antibiotics detection. This proposed approach features with several aspects. Firstly, the release of the two split G-rich parts relies on target-induced enzyme-assisted cascade reaction, which effectively improves the specificity and S/N of this biosensor. Secondly, by taking advantage of DNAzyme as catalytic tag, label-free electrochemical strategy can be achieved, which avoids the labeling of electroactive reporter and decreases the analysis cost. Moreover, by replacing antibiotic aptamer with the corresponding DNA substrates for target recognition, this created label-free electrochemical biosensor can be ingenious applied for the detection of wide variety of analytes. Therefore, our electrochemical strategy provides a label-free, simple and universal platform for antibiotics detection and related food safety analysis.

2. Experimental

2.1 Materials and reagents

Kanamycin and other antibiotics including tetracycline, streptomycin, oxytetracycline, tobramycin, ampicillin together with dimethyl sulfoxide (DMSO) and 6-mercapto-l-hexanol (MCH) were obtained from Aladdin Chemistry Co. Ltd. (Shanghai, China). Exonuclease III and the endonuclease *Nt.BbvCI* were purchased from New England Biolabs Inc. (Beijing, China). Hemin and hydrogen peroxide (H_2O_2) were ordered from Sigma Aldrich Chemical Co (St. Louis, MO, USA). The former was dissolved in DMSO to make the stock solution

View Article Online
DOI: 10.1039/C9AN00857H

(20 μM) and stored at -20°C to further use. Acryl/bis 30% solution (29:1), *N,N,N′,N′*-tetramethylethylenediamine (TEMED), ammonium persulfate, 10×TBS buffer (pH 7.4) and DNA ladder marker were obtained from Shanghai Sangon Biotech. Inc. (China). GelRed was purchased from Biotium. All oligonucleotides used in this work were HPLC-purified and synthesized by Sangon Biotechnology Co. Ltd (Shanghai, China). The sequences of oligonucleotides were introduced in **Table 1**. Other chemical reagents were ordered from Sinopharm Chemical Reagent Co. Ltd. (Beijing, China). All solutions were prepared using ultrapure water with an electric resistance > 18.25 MΩ·cm, which was obtained through a Millipore Milli-Q water purification system (Billerica, MA, USA). PBS (10 mM PB, 0.14 M NaCl, pH 7.4) was used during the experiments proceeding. Before the experiment, the equal bulk of aptamer (2 μM) and primer (2 μM) were mixed sufficiently, then the solution was incubated at 95°C for 5 min and cooled to indoor temperature to form double-arched probe. The underlined part of aptamer is matched with the primer. The underlined part of HP1 is recognition sequences for *Nt.BbvCI*, and the arrow indicated the nicking site. The underlined part of HP2 and HP3 are G1 and G2, respectively.

Table 1. Oligonucleotides sequences used in this study.

Oligonucleotide name	Sequence (5’ to 3’) description
Aptamer (Ap)	TGGGGGTTGAGGCTAAGCCGAC
Primer (Pr)	GGCTTAGCTGAGGACCCCCAAAAA
Hairpin probe1 (HP1)	ATCACAACGGTCC↓TCAGCTAGTGATAAA
Hairpin probe2 (HP2)	ACTAACCTCGTAGGGCGGGATGGGTACGAGGTTAGTCC GTTGTGAT

View Article Online
DOI: 10.1039/C9AN00857H

Hairpin probe3 (HP3)	GGGTAGGATCGAACAATCCTACCCATCACTAGCTGA
Capture probe (CP)	TGTTCGATCCTAATACGAGGTTAGTAAA-SH

2.2 Apparatus and measurements

Cyclic voltammetry (CV), differential pulse voltammetry (DPV) and electrochemical impedance spectra (EIS) were implemented with a CHI660D electrochemical workstation that bought from Shanghai Huachen Instrument Co. Ltd. Polyacrylamide gel electrophoresis (PAGE) electrophoresis was made using DYCZ-24DN electrophoresis cell (LIUYI, Beijing China) and Bio-Rad Gel imaging system (Bio-Rad, USA). A classical three-electrode system was applied in the research which consisted of Ag/AgCl electrode as reference electrode, platinum wire was used to the auxiliary electrode and the working electrode was gold electrode with the diameter of 2 mm. CV and EIS were performed in 5 mM $[Fe(CN)_6]^{3-/4-}$, including 0.25 M KCl. DPV was measured in PBS (10 mM, pH 7.4) containing 20 mM H_2O_2, the voltage range from -0.1 V to -0.55 V.

2.3 Gold electrode treatment and modification

Before the experiment, the working gold electrodes were polished meticulous with 0.3 and 0.05 mm alumina suspension. Next, these gold electrodes were immersed in freshly prepared piranha solution (H_2O_2/H_2SO_4, the volume ratio was 1:3) for 2 h, and then rinsed with ultrapure water thorough. Afterwards, these working electrodes were cleaned using of ultrasonic in the ethanol solution. Whereafter, in the process of electrode modification, 5 μL of CP solution (20 μM) was modified on the gold electrode by the Au-S bond for 2 h at 37°C. Then these electrodes were rinsed using PBS to get rid of the no adsorbed of CP. Afterwards, the gold electrodes were immersed into 2 mM MCH solution for 1 h to block the unoccupied

View Article Online
DOI: 10.1039/C9AN00857H

sites of the electrode and eliminate the nonspecific adsorption. Finally, these working electrodes were completely rinsed with PBS and stored at 4°C for ready.

2.4 Nt.BbvCI and Exo III-assisted cascade signal amplification

The details of the experiment were as follows: sample solution of 5 μL kanamycin (the final concentrations ranging from 0 to 1 nM), 2 μL aliquot of 1 μM double-arch probe, containing 2 μL buffer, 2 μL aliquot of 5 μM HP1 and 2 μL aliquot of 50 μM HP2, 2 μL aliquot of 50 μM HP3, 2 μL *Nt.BbvCI*, 3 μL Exo III, were mixed at 37°C for 2 h to perform the enzyme-assisted cascade amplification reactions.

2.5 Antibiotic detection

This above reaction product was dropped on the surface of modified gold electrode and reacted in a humid atmosphere at 37°C for 2 h. Then, we rinsed the electrode by PBS thoroughly aim to removing no paired G1 and G2. After the above operation completed, 5 μL of 20 μM hemin was dropped on the working electrode and incubated for 30 min to induce the two G-rich sequence to form DNAzyme. Finally, the response signal was measured by DPV in 15 mL of PBS (10 mM, pH 7.4) containing 20 mM H_2O_2.

2.6 PAGE analysis

The product of each step of was characterized using 20 % PAGE. In the PAGE assay, electrophoresis was carried out at 100 V in 1 × TBE (50 mM Tris Borate, 2.0 mM EDTA, pH 8.2) buffer for 90 min at room temperature and stained for 30 min in a 1 × GelRed solution. The imaging of resulting gel was photographed by the gel imaging system under ultraviolet light.

3. Results and discussion

View Article Online
DOI: 10.1039/C9AN00857H

3.1 Principle of the electrochemical strategy

The **Scheme1** demonstrates the working principle of the electrochemical biosensor for detecting kanamycin. Our system contains a double-arch probe combined with aptamer (Ap) and primer (Pr), three hairpin probes, a capture probe (CP), nicking endonuclease (*Nt.BbvCI*) and exonuclease III (Exo III). In the presence of target kanamycin, it specifically binds to the Ap, leading in the release of Pr which can anneal with the HP1 and forming specific double-stranded sequence is recognized by *Nt.BbvCI.* With the help of *Nt.BbvCI*, HP1 is divided into trigger 1 (Tr1) and trigger 2 (Tr2), releasing the Pr. Meanwhile, the free Pr continues to open the remaining HP1 and initiating a new *Nt.BbvCI*-assisted amplification reaction. It is worth mentioning that hairpin probe 2 (HP2) and hairpin probe 3 (HP3) are skillfully designed to include three GGG repeat-inserted sequence (G1) and one GGG repeats-inserted parts (G2) as well as can hybridize with Tr1 and Tr2 to produce a DNA duplex from the 3'-terminus. The Exo III has the function that cleaves duplex DNA from blunt or recessed 3'-terminus, so HP2 and HP3 are digested, generating G1 and G2. Meanwhile, the released Tr1 and Tr2 can hybridize with another HP2 and HP3, resulting in the degradation of HP2 and HP3, the generation of G1 and G2. Obviously, after the above enzyme-assisted cascade amplification reaction, a small amount of target can produce innumerable G1 and G2 in the system. The CP, with a thiol group labeled at 3' end, immobilizes on electrode surface by Au-S interaction and includes paired sequence with G1 and G2. When the reaction product is dropped on the working electrode surface, G1 and G2 will be infinitely close, thus generating assembly of G-quadruplex/hemin structure when hemin and K^+ are present. As is well known, the complex can be used as HRP-mimicking

View Article Online
DOI: 10.1039/C9AN00857H

DNAzyme and catalyze the reduction of H_2O_2, thus a significantly strong current signal is observed. The mechanism of DNAzyme catalyzing H_2O_2 can be seen as following inset in Scheme1. The gold electrode is considered as an electron donor. By the combination of target-induced enzyme-assisted cascade reaction and split G-quadruplex DNAzyme, the designed strategy offers a simple, versatile and practical electrochemical platform for detecting antibiotics with high specificity and sensitivity.

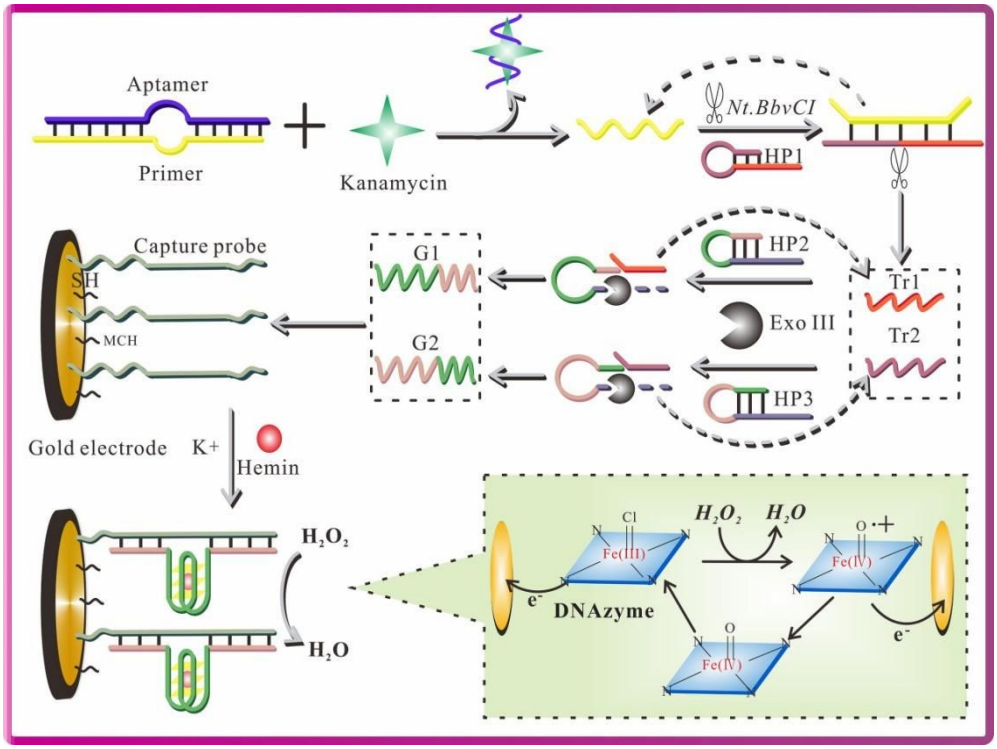

Scheme 1. Schematic illustration of the electrochemical biosensor for kanamycin detection.

3.2 Feasibility analysis of the biosensor

In order to verify the feasibility of proposed electrochemical biosensor for detecting kanamycin, several control experiments were implemented under different conditions, as depicted in **Fig. 1**. For the positive sample, a prominent DPV peak was observed in -0.35 V, manifesting this system generates a large number of split G-quadruplex DNAzyme (curve a). Adversely, there was a weak current peak for the blank sample (curve b). This comparison

View Article Online
DOI: 10.1039/C9AN00857H

explicitly revealed that the operation of electrochemical biosensor depended on kanamycin-aptamer interaction. Moreover, when kanamycin was replaced by tetracycline, an almost invisible current signal was obtained, proving the high specificity of this electrochemical strategy for target kanamycin detection (curve c). When there was no *Nt.BbvCI* in solution, we also found a negligible current peak in the curve which showed the *Nt.BbvCI* was an essential element for the formation of G-quadruplex/hemin (curve d). Furthermore, when the electrode surface was not modified with the CP, it was observed that a very tidy current signal (curve e), implying the CP was an indispensable condition for forming spilt G-quadruplex DNAzyme. In summary, it was consciously considered that our biosensor could be used to detect kanamycin.

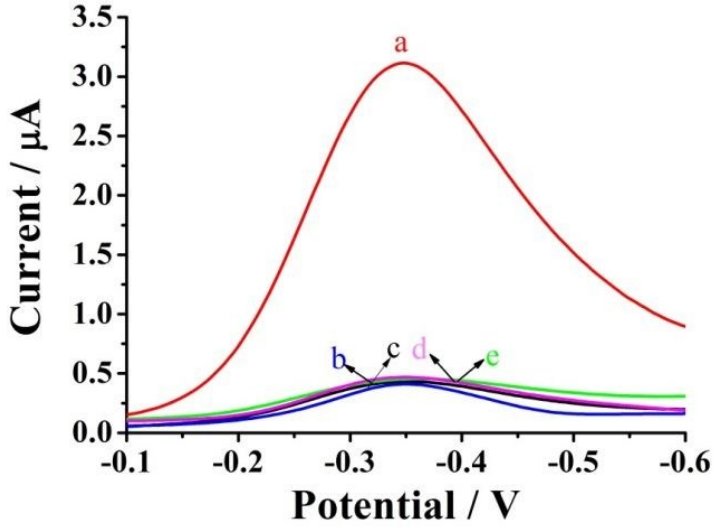

Fig. 1. DPV responses of the biosensor through analyze 1 nM kanamycin (a). Curves b to e were for the control experiments which were performed with no target kanamycin (b), kanamycin was replaced by 1 nM non-target tetracycline (c), 1 nM kanamycin without *Nt.BbvCI* (d), 1 nM kanamycin without no CP (e).

3.3 PAGE characterization of the cascade enzymatic amplification reaction.

As can be seen from Fig 2, we can see more direct evidence of the biosensor through

View Article Online
DOI: 10.1039/C9AN00857H

PAGE analysis. The double-arch probe, HP1, HP2, HP3 and CP displayed an individual clear band in the image, respectively (from lane 1 to lane 5). After incubation with target, we found a new band higher the HP1 and double-arch probe appear (lane 6), indicating the formation of Pr-HP1. Further, with the disappearance of Pr-HP1, a new band with low molecular weight was appeared in the image (lane 7), demonstrating abundant G1 and G2 produced on account of enzyme-assisted cascade amplification reaction. For positive samples, compared with the lane 7, the G1 and G2 disappeared, at the same time, a new band with high molecular weight was observed (lane 8), suggesting the CP combined with G1 and G2 ,that was the generation of a great number of spilt-G-quadruplex structure. In contrast, several bright bands with the same mobility as that of double-arch probe, HP1 HP2 HP3 and CP were observed for the blank sample (lane 9). These results revealed that the forming of spilt-G-quadruplex relied on the specific binding between kanamycin and aptamer.

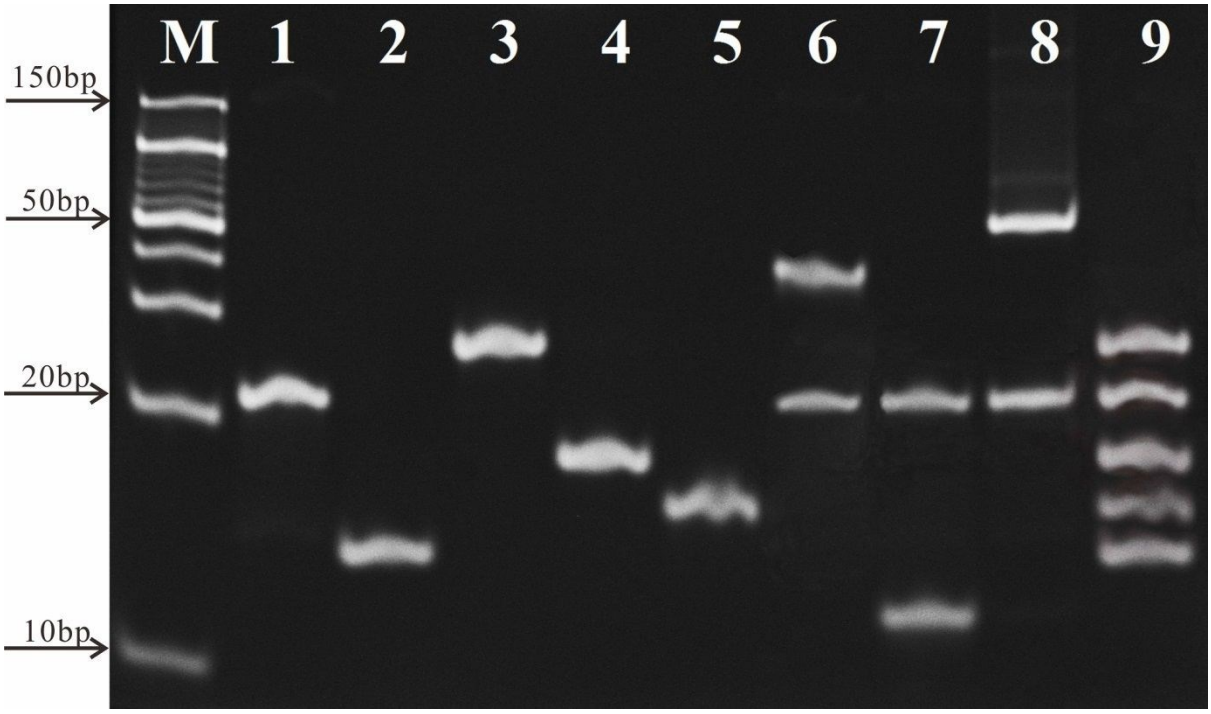

Fig. 2. PAGE images for electrochemical reaction. Lane M, DNA marker; Lane 1, double-arch probe; Lane 2, HP1; Lane 3, HP2; Lane 4, HP3; Lane 5, CP; Lane 6, target,

View Article Online
DOI: 10.1039/C9AN00857H

double-arch probe and HP1; Lane 7, target, double-arch probe, HP1, HP2, HP3, *Nt.BbvCI*, Exo III; Lane 8, positive sample; Lane 9, blank sample.

3.4 Electrochemical characterization of the modified electrodes

We used the classical techniques of cyclic voltammetry (CV) and electrochemical impedance spectra (EIS) to capture the changes in the process of modification on the working electrode surface. As depicted in Fig. 3A, a couple of distinctly redox peaks was monitored at 0.17 V and 0.30 V due to the excellent electrical conductivity (curve a). After modifying CP on the surface of gold electrode, the current peak evidently decreased which indicated the oligonucleotides hinder the access of $[Fe(CN)_6]^{3-/4-}$ on the electrode surfaces (curve b). As non-specific sites were blocked by MCH, the peak of CV continued to weaken (curve c). After the incubation of the modified electrode with the positive sample, a prominent lower current signal was observed (curve d), manifesting this electrochemical biosensor based on enzyme-assisted cascade amplification generates abundant G1 and G2, which were bound to electrode surface, so the electron transport efficiency on electrode interface was further reduced. All of the above changes were concerned to the negatively charged phosphate skeleton of the immobilized DNA molecule and MCH could obstruct negatively charged $[Fe(CN)_6]^{3-/4-}$ close to the electrode surface.

Meanwhile, EIS was applied in monitoring the characterization of surface-modified electrodes in Fig.3B. The semicircle diameter was equal to electron-transfer resistance (R_{et}). The bare electrode showed the good conductivity (curve a). After the CP was modified on the bare electrode, the R_{et} increased obviously, because the negatively charged DNA molecule blocks the electron transfer on electrode surface (curve b). Then, the R_{et} continued to increase

View Article Online
DOI: 10.1039/C9AN00857H

after the MCH was decorated on the electrode (curve c). Next the modified electrode was incubated with 1 nM kanamycin, the R_{et} further increased (curve d). The EIS changes were agreement with the CV responses, which gave indirect evidence that the electrochemical biosensor interface was successfully constructed.

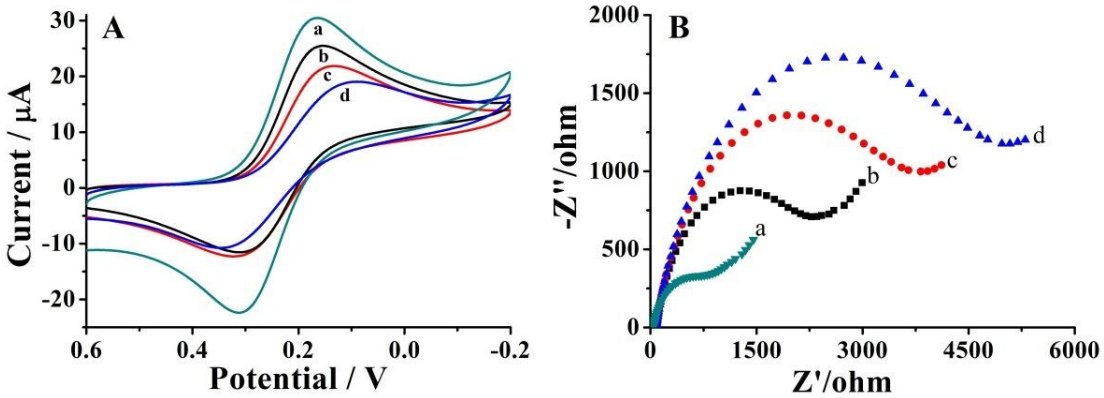

Fig. 3. CVs (A) and EIS (B) showed the modification process on the gold electrode. bare Au electrode (a), CP/Au (b), MCH/CP/Au (c), and the modified electrode upon analyzing 1 nM kanamycin (d). CV and EIS measurements were performed in containing 0.25 mM KCl and 5.0 mM K_3 [Fe $(CN)_6$].

3.5 Optimization of experimental conditions

Before quantitative detection of kanamycin by the electrochemical biosensor assay, these experiment conditions, including the incubation time of hemin, the concentrations of Exo III and H_2O_2, the molar ratio of HP1 and HP2, were discussed. As shown in Fig. 4A, it was observed that the current intensities for the positive sample increased continuously with the increase of the incubation time of hemin until a plateau was reached at 30 min (curve a). Conversely, there was no obvious change in the intensity of the current peak of the blank sample (curve b). So, the 30 min was used as the optimum the incubation time of hemin. Exo III was an indispensable element to enzyme-assisted cascade amplification. The

View Article Online
DOI: 10.1039/C9AN00857H

concentration of Exo III was tested from 0 to 25 U in Fig. 4B. As we can see, the current response of positive samples achieved a plateau after 15 U (curve a), the DPV peak of the blank sample didn't change (curve b). There, 15 U was selected as optimized concentration in the subsequent experiments. The H_2O_2 played an important role in experiment analysis. Thus, we studied the relationship between concentration of H_2O_2 and the $(I_1\text{-}I_0)/I_0$ values. I_1 and I_0 represented the DPV peak intensity in the presence and absence of 1 nM kanamycin, respectively. As can be seen from Fig. 4C, the $(I_1\text{-}I_0)/I_0$ values increased with the elevated concentration of H_2O_2 and reached the saturated status after 20 mM, so we selected 20 mM as the optimal concentration of the H_2O_2. In addition, the molar ratio of HP1 and HP2 was essential for the amplification efficiency of this electrochemical biosensor. So, in Fig. 4D, we obtained a fast increase in the current upon the elevation of when the molar ratio of HP1 and HP2 from 1:1 to 1:10. But further beyond the ratio of 1:10 couldn't make the rise of DPV response and S/N. For the blank sample, the DPV response showed ignorable enhance with the increase of the molar ratios. Thus, 1:10 was selected the optimal the ratio of HP1 and HP2 in the following experiments.

View Article Online
DOI: 10.1039/C9AN00857H

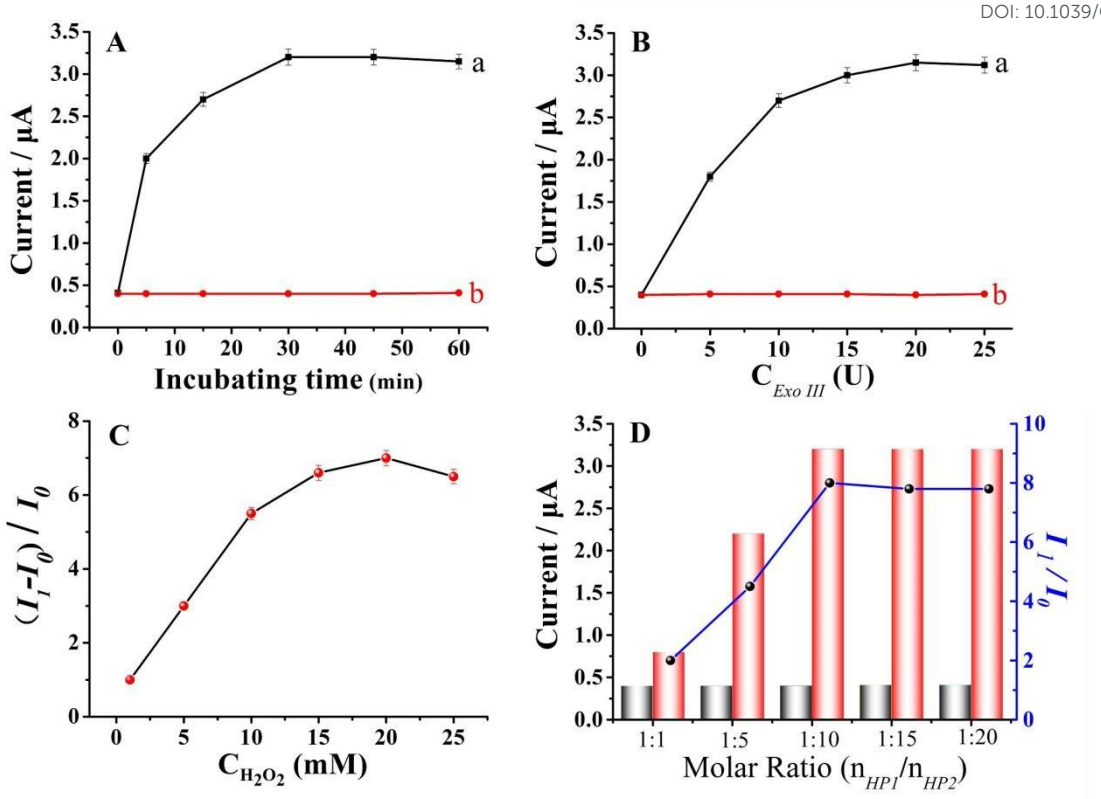

Fig. 4. (A) Effect of the incubation time of hemin on the current response intensity of the electrochemical biosensor in the presence (curve a) and absence (curve b) of 1 nM kanamycin; (B) Effect of different concentrations of Exo III on the DPV response when the target is present (curve a) and absent (curve b) of 1 nM kanamycin; (C) Effect of the concentration H_2O_2 to DPV peak intensities; (D) Effect of the molar ratio of HP1 and HP2 to current peak of the electrochemical biosensor in the presence (the red bar) and absence (the black bar) of 1 nM kanamycin. Error bars are standard deviations across three repetitive experiments.

3.6 Analytical performance of the electrochemical biosensor for detecting kanamycin

For researching the performance of the biosensor, various concentrations of kanamycin were monitored under the above optimal conditions. Fig. 5A showed the DPV intensities of the electrochemical platform to different kanamycin concentrations. It was observed that the

View Article Online
DOI: 10.1039/C9AN00857H

DPV signal intensities increased with the increasing concentration of kanamycin from 0 to 1 nM. According to the inset of the Fig. 5B, we found that the current response was proportional to the logarithmic concentration of kanamycin which over 4 orders of magnitude (from 100 fM to 1 nM) with the equation of I (μA) = 1.22478+0.6252lg ($C_{kanamycin}$/pM) (R=0.998), and the limit of detection (LOD) was calculated to be 83 fM in terms of the rule of 3 times standard deviation over the blank response. At the same time, we listed other detection method for kanamycin in **Table 2**. Compared with other methods, our strategy showed a wider linear range and a lower LOD, which should be attributed to the efficient enzyme-assisted cascade amplification reaction coupled with spilt G-quadruplex DNAzyme strategy.

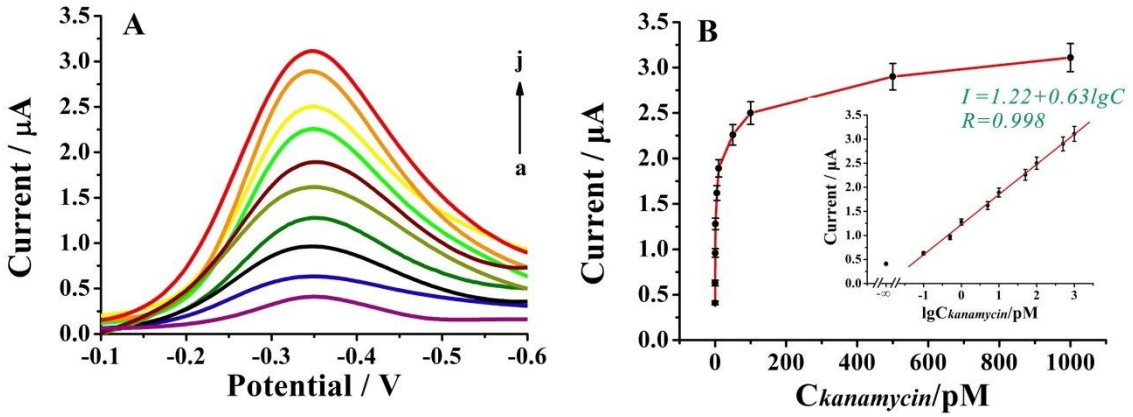

Fig. 5. (A) DPV responses of the biosensor toward kanamycin with different concentrations (from curve a to j: 0, 100 fM, 500 fM, 1 pM, 5 pM, 10 pM, 50 pM 100 pM, 500 pM, 1 nM, respectively); (B) Variance of DPV intensity as a function of kanamycin with various concentrations. Inset: the calibration curve of DPV peak current versus the logarithm of kanamycin in range from 0 to 1 nM. Error bars show the standard deviations across three repetitive experiments.

Table 2. Comparison of different assay methods for kanamycin determination.

View Article Online
DOI: 10.1039/C9AN00857H

Detection method	Detection range	Detection limit	Reference
SERS	1 nM-100 nM	0.75 nM	14
SPR	100 nM-10 μM	43 nM	16
FRET	1 nM-80 nM	0.29 nM	17
Colorimetry	50 pM-500 pM	14.7 pM	33
Fluorescence	24.75nM-137.15nM	7.5 nM	34
HPLC	10 nM-150 nM	25 nM	35
ELISA	1.7 pM-3.4 pM	7.7 pM	36
Luminescence	0.2 μM-150 μM	14.3 nM	37
Microchip electrophoresis	12.8 μM-112 uM	2.1 μM	38
Electrochemistry	1 nM to 10 mM	1 nM	39
Electrochemistry	1 pM to 10 nM	0.5 pM	40
Electrochemistry	100 fM-1 nM	83 fM	this work

3.7 Specificity of the biosensor

The specificity of the enzyme-assisted cascade signal amplification electrochemical method coupled with split G-quadruplex DNAzyme was testified through current peak distinction of target kanamycin and various non-target antibiotics containing ampicillin, terramycin, carbenicillin, oxytetracycline chloramphenicol. As shown in **Fig. 6**, the DPV responses for the non-targets sample were all weak although the concentration was 10-fold greater over the target. These consequences proved that the electrochemical biosensor had an excellent specific recognition for kanamycin against other interfering antibiotics.

View Article Online
DOI: 10.1039/C9AN00857H

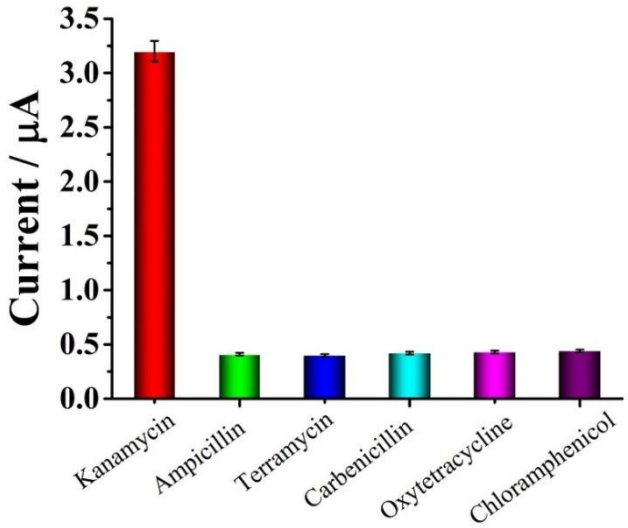

Fig. 6. DPV responses acquired by the biosensor for different antibiotics detection. The concentration of kanamycin is 1 nM, other non-target antibiotics are 10 nM. Error bars are standard deviations across three repetitive experiments.

3.8 Real sample analysis

To further test the applicability of the electrochemical biosensor in real samples, the kanamycin was monitored using our method in spiked milk. Different concentrations of kanamycin were added directly to the standard milk sample and detected without any pretreatment except for dilution with a buffer solution. We also used the classical ELISA method to detect these spiked samples and compared with these results measured by our constructed biosensor in **Table 3**. We observed these results obtained by our biosensor were good consistent with those obtained via the ELISA method, and the discrepancies between the two methods were all smaller than 10.6%. Besides, the recovery of our biosensor was in the range of 95.7%-104.8%, which can be confirmed that the actual results and theoretical expectation are approximately identical. These results implied that the designed strategy has a splendid potential for monitoring kanamycin in real sample with excellent accuracy and reproducibility.

View Article Online
DOI: 10.1039/C9AN00857H

Table 3. Comparison of the biosensor assay and ELISA to detect kanamycin in milk.

Spiked amount	Measured (pM)		Recovery (%)±SD, n=5	
(pM)	biosensor	ELISA	biosensor	ELISA
1.000×10^{-1}	$(1.022\pm0.044)\times10^{-1}$	$(1.041\pm0.018)\times10^{-1}$	102.2±4.4	104.1±1.8
1.000×10^{0}	$(1.036\pm0.012)\times10^{0}$	$(1.066\pm0.034)\times10^{0}$	103.6±1.2	106.6±3.4
1.000×10^{1}	$(1.024\pm0.022)\times10^{1}$	$(0.977\pm0.037)\times10^{1}$	102.4±2.2	97.7±3.7
1.000×10^{2}	$(0.985\pm0.017)\times10^{2}$	$(1.031\pm0.034)\times10^{2}$	98.5±1.7	103.1±3.4
1.000×10^{3}	$(0.976\pm0.019)\times10^{3}$	$(0.963\pm0.041)\times10^{3}$	97.6±1.9	96.3±4.1

4. Conclusion

In summary, we have constructed a label-free, simple and efficient electrochemical biosensor for high S/N detection of kanamycin based on enzyme-assisted cascade amplification coupled with split G-quadruplex DNAzyme. In this work, the two G-rich oligonucleotide sequences were caged into two hairpin probes, respectively, eliminating the possibility of assembling into active peroxidase DNAzyme when the kanamycin was absent, thus high S/N detection of target could be achieved. To the best of our knowledge, this is the first time that split G-quadruplex DNAzyme has been used to electrochemical field for antibiotics detection, and the LOD achieved as low as 83 fM. Besides, we applied this biosensor to detect kanamycin in the actual sample, further verified its practicality. Therefore, the ingenious method has a potential to provide a versatile and practical electrochemical platform for detecting small molecules and related food safety analysis.

View Article Online
DOI: 10.1039/C9AN00857H

Acknowledgements

This work was supported by National Natural Science Foundation of China (31471644), the Primary Research & Development Plan of Shandong Province (2017GSF220009), program for Taishan Scholer of Shandong provinces (ts201712048), University of Jinan Scientific Research Fund (Youth Project XKY1421) and the Doctoral Fundation of University of Jinan (XBS1431).

References

1. J. Liu, J. Zeng, Y. Tian and N. Zhou, *Analyst*, 2017, **143**, 182-189.

2. B. Wang, X. L. Lv, D. Feng, L. H. Xie, J. Zhang, M. Li, Y. Xie, J. R. Li and H. C. Zhou, *J Am Chem Soc*, 2016, **138**, 6204-6216.

3. P. Xing, D. Wu, J. Chen, J. Song, C. Mao, Y. Gao and H. Niu, *Analyst*, 2019, **144**, 2656-2661.

4. X. He, Y. Xu, J. Chen, J. Ling, Y. Li, L. Huang, X. Zhou, L. Zheng and G. Xie, *Water Res*, 2017, **124**, 39-48.

5. A. Sharma, G. Istamboulie, A. Hayat, G. Catanante, S. Bhand and J. L. Marty, *Sensor Actuat B: Chem*, 2017, **245**, 507-515.

6. O. Genilloud, *Nat Prod Rep*, 2017, **34**, 1203-1232.

7. J. C. G. Sousa, A. R. Ribeiro, M. O. Barbosa, M. F. R. Pereira and A. M. T. Silva, *J Hazard Mater*, 2018, **344**, 146-162.

8. S. Han, B. Li, Z. Song, S. Pan, Z. Zhang, H. Yao, S. Zhu and G. Xu, *Analyst*, 2016, **142**, 218-223.

9. B. Jia, A. R. Raphenya, B. Alcock, N. Waglechner, P. Guo, K. K. Tsang, B. A. Lago, B.

M. Dave, S. Pereira, A. N. Sharma, S. Doshi, M. Courtot, R. Lo, L. E. Williams, J. G. Frye, T. Elsayegh, D. Sardar, E. L. Westman, A. C. Pawlowski, T. A. Johnson, F. S. Brinkman, G. D. Wright and A. G. McArthur, *Nucleic Acids Res*, 2017, **45**, D566-D573.

10. L. He, Z. Shen, Y. Cao, T. Li, D. Wu, Y. Dong and N. Gan, *Analyst*, 2019, **144**, 2755-2764.

11. B. C. McWhinney, S. C. Wallis, T. Hillister, J. A. Roberts, J. Lipman and J. P. Ungerer, *J Chromatogr B*, 2010, **878**, 2039-2043.

12. X.-H. Zhang, Y. Deng, M.-Z. Zhao, Y.-L. Zhou and X.-X. Zhang, *Rsc Adv*, 2018, **8**, 4063-4071.

13. W. Jiang, Z. Wang, R. C. Beier, H. Jiang, Y. Wu and J. Shen, *Anal Chem*, 2013, **85**, 1995-1999.

14. A. H. Nguyen, X. Ma, H. G. Park and S. J. Sim, *Sensor Actuat B: Chem*, 2019, **282**, 765-773.

15. Q. Fang, Y. Li, X. Miao, Y. Zhang, J. Yan, T. Yu and J. Liu, *Analyst*, 2019, **144**, 3649-3658.

16. L. Zhang, C. Zhu, C. Chen, S. Zhu, J. Zhou, M. Wang and P. Shang, *Food Chem*, 2018, **266**, 170-174.

17. S. Dehghani, N. M. Danesh, M. Ramezani, M. Alibolandi, P. Lavaee, M. Nejabat, K. Abnous and S. M. Taghdisi, *Anal Chim Acta*, 2018, **1030**, 142-147.

18. J. Liu, Z. Cao and Y. Lu, *Chem Rev*, 2009, **109**, 1948-1998

19. J. Liu and Y. Lu, *J Am Chem Soc*, 2003, **125**, 6642-6643.

20. Y. Yao, X. Wang, W. Duan and F. Li, *Analyst*, 2018, **143**, 709-714.

21. S. M. Taghdisi, N. M. Danesh, M. A. Nameghi, M. Ramezani, M. Alibolandi and K. Abnous, *Biosens Bioelectron*, 2019, **133**, 230-235.

22. M. Zhou, X. Teng, Y. Li, R. Deng and J. Li, *Anal Chem*, 2019, **91**, 5295-5302.

23. S. Roy, S. P. Hennelly, H. Lammert, J. N. Onuchic and K. Y. Sanbonmatsu, *Nucleic Acids Res*, 2019, **47**, 3158-3170.

24. Z. Chen, C. Wang, L. Hao, R. Gao, F. Li and S. Liu, *Biosens Bioelectron*, 2019, **128**, 104-112.

25. J. Zhang, L. L. Wang, M. F. Hou, Y. K. Xia, W. H. He, A. Yan, Y. P. Weng, L. P. Zeng and J. H. Chen, *Biosens Bioelectron*, 2018, **102**, 33-40.

26. X. Song, Y. Wang, S. Liu, X. Zhang, H. Wang, J. Wang and J. Huang, *Analyst*, 2018, **143**, 5771-5778.

27. Y. Xiong, M. Liang, Y. Cheng, J. Zou and Y. Li, *Analyst*, 2018, **144**, 161-171.

28. Q. Li, D. Zhou, J. Pan, Z. Liu and J. Chen, *Analyst*, 2018, **143**, 5670-5675.

29. H. Cheng, X. Qiu, X. Zhao, W. Meng, D. Huo and H. Wei, *Anal Chem*, 2016, **88**, 2937-2943.

30. Y. Guo, Y. Wang, S. Liu, J. Yu, H. Wang, Y. Wang and J. Huang, *Biosens Bioelectron*, 2016, **75**, 315-319.

31. K. Zhang, S. Lv, M. Lu and D. Tang, *Biosens Bioelectron*, 2018, **117**, 590-596.

32. L. Zhou, X. Shen, N. Sun, K. Wang, Y. Zhang and R. Pei, *Analyst*, 2015, **140**, 5450-5453.

33. X. Cui, R. Li, X. Liu, J. Wang, X. Leng, X. Song, Q. Pei, Y. Wang, S. Liu and J. Huang, *Anal Chim Acta*, 2018, **997**, 1-8.

34. J. Deng, Y. Liu, X. Lin, Y. Lyu, P. Qian and S. Wang, *Sensor Actuat B: Chem*, 2018, **273**, 1495-1500.

35. B. Blanchaert, E. Poderós Jorge, P. Jankovics, E. Adams and A. Van Schepdael, *Chromatographia*, 2013, **76**, 1505-1512.

36. J. He, Y. Wang and X. Zhang, *Food Anal Method*, 2015, **9**, 744-751.

37. K.-H. Leung, H.-Z. He, D. S.-H. Chan, W.-C. Fu, C.-H. Leung and D.-L. Ma, *Sensor Actuat B: Chem*, 2013, **177**, 487-492.

38. K. C. Chong, L. Y. Thang, J. P. Quirino and H. H. See, *J Chromatogr A*, 2017, **1485**, 142-146.

39. R. Liu, Z. Yang, Q. Guo, J. Zhao, J. Ma, Q. Kang, Y. Tang, Y. Xue, X. Lou and M. He, *Electrochimica Acta*, 2015, **182**, 516-523.

40. C. Han, R. Li, H. Li, S. Liu, C. Xu, J. Wang, Y. Wang and J. Huang, *Microchimica Acta*, 2017, **184**, 2941-2948.